



AUTHORS:

Pogisego Dinake¹
Gothatamang N. Phokedi¹
Mbhatsi M. Keetile¹
Mmamiki A. Bothomilwe¹
Mogomotsi Tlhako¹
Bokang Present²
Janes Mokgadi^{1,3}
Rosemary Kelebemang^{1,4}

AFFILIATIONS:

¹Department of Chemical and Forensic Sciences, Botswana International University of Science and Technology, Palapye, Botswana
²Department of Physics and Astronomy, Botswana International University of Science and Technology, Palapye, Botswana
³Chemical, Biological Nuclear and Radiological Weapons Management Authority, Ministry of Defence, Justice and Security, Gaborone, Botswana
⁴National Environmental Laboratory, Department of Waste Management and Pollution Control, Gaborone, Botswana

CORRESPONDENCE TO:

Pogisego Dinake

EMAIL:

dinakep@biust.ac.bw

DATES:

Received: 11 May 2022

Revised: 07 Feb. 2023

Accepted: 09 Feb. 2023

Published: 28 Sep. 2023

HOW TO CITE:

Dinake P, Phokedi GN, Keetile MM, Bothomilwe MA, Tlhako M, Present B, et al. One-pot hydrothermal green synthetic approach of fluorescent carbon dots as optical probes for 2-nitrophenol. *S Afr J Sci.* 2023;119(9/10), Art. #13921. <https://doi.org/10.17159/sajs.2023/13921>

ARTICLE INCLUDES:

- Peer review
- Supplementary material

DATA AVAILABILITY:

- Open data set
- All data included
- On request from author(s)
- Not available
- Not applicable

EDITORS:

Priscilla Baker
Amanda-Lee Manicum

KEYWORDS:

2-nitrophenol, fluorescence, carbon dots, green synthesis, biomass, *Citrullus vulgaris*

FUNDING:

Botswana International University of Science and Technology (BIUST/ds/R&I/26/2016)

One-pot hydrothermal green synthetic approach of fluorescent carbon dots as optical probes for 2-nitrophenol

The pursuit of a cost-effective and green synthetic approach to chemical sensors and their application in the sensing of toxic and harmful substances is a never-ending exercise for scientists and researchers. Preparation of fluorescent carbon dots (C-dots) from biomass using water as a solvent and a hydrothermal autoclave to provide the required synthesis temperature offers a cheap and environmentally friendly synthetic approach. Herein, we report a faster, less costly and ecofriendly hydrothermal synthetic approach of carbon dots from *Citrullus vulgaris* peels as a precursor. The as-prepared carbon dots exhibited hydroxyl, carbonyl and amide functional groups on the surface and an amorphous structure with a particle size distribution of 1.7–3.0 nm. Moreover, the carbon dots displayed intense blue emission fluorescence at 470 nm after excitation at 400 nm. The as-prepared carbon dots demonstrated effective application without further modification towards the selective and sensitive optical recognition of 2-nitrophenol used in the manufacture of explosives. A limit of detection of 2.28×10^{-7} M was achieved, and no fluorescence quenching was observed in the presence of other nitroaromatic and benzene derivatives indicating excellent selectivity towards 2-nitrophenol. Finally, further studies are required to investigate the potential for the as-prepared carbon dots to monitor nitroaromatic pollutants in real environmental systems.

Significance:

- Terrorism is an ever-increasing problem, and law enforcement agencies are continuously searching for and detecting explosives hidden in travel luggage, mail packages, vehicles and aircrafts using sophisticated equipment which are not available in developing countries such as Botswana.
- This work unveils a facile and environmentally friendly approach towards the detection of 2-nitrophenol used in the manufacture of explosives by employing highly luminescent C-dots obtained from locally available agricultural waste.
- The utilisation of agricultural waste can help advance a sustainable waste management programme and promote a circular economy.

Introduction

Terrorism is an ever-increasing problem due to an array of chemicals that can be employed as precursors in the manufacture of explosives.¹ Human social security is under constant threat due to a surge in well-organised and sophisticated terrorist bomb attacks. Law enforcement and security officers are continuously searching for and detecting hidden explosives in travellers, travel luggage, mail packages, vehicles and aircrafts. Therefore, analytical field and laboratory detection and unearthing of explosives are of utmost importance in bomb neutralisation and protection of lives and property.² Nitroaromatic compounds are common major components of explosives.³ Their substantial use has resulted in the release of elevated levels of these organic compounds into the environment leading to pollution of soil and water.⁴ Additionally, the nitroaromatic compounds are poorly biodegradable, highly stable and result in adverse health effects in humans due to their toxicity.⁵ Nitroaromatic compounds such as 2-nitrophenol (2-NP) are not only used in the manufacture of explosives but have also found extensive use in the production of pesticides, herbicides, insecticides, dyes, rubber chemicals, textile, petroleum solvents, pharmaceuticals and as intermediates in the synthesis of other chemicals.⁶ The hydrolysis of 2-NP containing explosive residues results in the release of 2-NP into the environment causing contamination of the environment and public health risk owing to its acute toxicity and mutagenic capabilities.⁷ The adverse health effects associated with exposure to 2-NP include kidney and liver damage, cancer and blood disorder.⁸ As a result, 2-NP has been included in the United States Environmental Protection Agency (USEPA) list of priority pollutants owing to its carcinogenic and bioaccumulation effects.⁹ On account of its highly toxic effects, this nitroaromatic compound has a maximum contaminant limit (MCL) of 4.8 µg/L as set by the USEPA.¹⁰ Therefore, it is of paramount importance that highly sensitive and selective methods are available for the low-level detection of this toxic organic chemical.

Presently, various conventional methods and techniques have been applied in the analysis of 2-NP such as chromatography, electrochemistry and spectroscopic techniques.^{11–13} Regrettably, these techniques generally require sophisticated and costly equipment accompanied by complex sample preparation and pre-treatment steps that are time consuming.⁶ Some of these methods lack low analyte discriminating ability towards nitroaromatic isomers such as 4-nitrophenol, 2-nitrophenol and 3-nitrophenol which restricts their broad utilisation.

This has necessitated scientists and researchers to continuously search for new methods and techniques that are not only cost effective but also sensitive and selective towards 2-NP. Amidst these several techniques, photoluminescence has been extensively explored owing to its simplicity and high sensitivity. Another important attribute of luminescent-based recognition and sensing techniques is the capability to detect explosives from



afar.² A great number of studies have been carried out on changes in the photoluminescence properties of certain substances upon exposure to 2-NP. For example, in a study by Chaudhary et al. 2019, fluorescent europium oxide (Eu_2O_3) nanoparticles that were surface modified with (3-aminopropyl)triethoxysilane (APTES) successfully detected 2-NP in aqueous media achieving detection limits of 4.6×10^{-6} M.¹⁴ The optical recognition of 2-NP was based on fluorescence quenching of the Eu_2O_3 nanoparticles by the 2-NP. The mechanism of this interaction involves donor-acceptor interaction between the electron-deficient 2-NP and the electron-rich primary amines on the surfaces of the Eu_2O_3 nanoparticles leading to the formation of Meisenheimer complexes (MHCs).¹⁴ In a similar study, luminescent silicon nanoparticles based on *N*-[3-(trimethoxysilyl) propyl]-ethylenediamine (DAMO) and functionalised with dopamine moiety were used for selective detection of 2-NP in the presence of other nitroaromatic compounds such as 3-nitrophenol, 4-nitrophenol, 2,4-dinitrophenol, 2,4,6-trinitrophenol, nitrotoluene, 3,5-dinitrobenzoic acid, 2,4-dinitrotoluene, *p*-nitrobenzoic acid, 1,3-dinitrobenzene, 2,4,6-trinitrotoluene, nitrobenzene and metal cations such as Cu^{2+} , Zn^{2+} , Mn^{2+} , Al^{3+} , K^+ , Ca^{2+} , Mg^{2+} and Ba^{2+} .⁶ A detection limit of 2.9×10^{-8} M was achieved for sensing of 2-NP using the luminescent silicon nanoparticles. Photoluminescent quantum dots doped containing heavy metals have also been applied as optical probes for nitroaromatic compounds such as 2-NP.^{15,16} Liu and co-workers have investigated the use of fluorescent hybrid copper (I) iodine cluster-based sensor ($[\text{Cu}_4\text{I}_4(\text{RTBT})_4]$, where ETBT is 2-ethylbenzo[d]thiazole) for optical recognition of 2-NP in aqueous media achieving high selectivity and low detection limits of 2.3×10^{-6} M.¹⁷ Similarly, Uddin et al.¹⁵ utilised modified glassy carbon electrode bearing ZnO/RuO_2 nanoparticles for the ultrasensitive and excellent selective detection of 2-NP with a detection limit of 5.22×10^{-13} M. Even though the use of luminescent quantum dots has been found to be efficient and effective as sensitive optical probes for 2-NP, they have rather shown some unappealing attributes such as high toxicity due to the use of toxic metals and solvents, high cost of starting materials and laborious preparation processes.¹⁶ Therefore, there is a continuous need to develop rapid, sensitive and selective methods that are simple and cost effective for the detection of 2-NP.

The discovery of carbon dots (C-dots) in 2004 has brought about a new perspective in chemical sensors and the attention of scientists and researchers has shifted towards exploiting the photoluminescence properties of these carbon nanomaterials.¹⁸ C-dots possess fascinating photoluminescent characteristics that are controlled by their size, shape, defects and surface functionalisation.¹⁹ The massive interest in carbon dots is believed to stem from the ease of their preparation from abundant precursors, functionalisation, low cost, low toxicity, biodegradability, tunable optical properties, biocompatibility, high chemical and photostability, excellent water solubility and immense potential for considerable applications.²⁰ This broad spectrum of attractive properties of carbon dots has resulted in their versatile application potential such as chemical sensing, drug delivery, catalysis, bioimaging and forensic applications.²¹⁻²⁵ To reap the full benefits of carbon dots, scientists and researchers are continuously searching for cheaper methods with high specificity and excellent yields for their synthesis. Two synthetic pathways have been exploited in the preparation of carbon dots, being the top-down and bottom-up approaches.²⁶ The top-down strategy employs the preparation of C-dots from the breakdown of large carbon source precursors such as multi-walled carbon nanotubes (MWCNTs), carbon fibres and graphite under aggressive physical or chemical reaction conditions.²⁷ In contrast, bottom-up synthetic strategies involve flexible synthesis procedures that can be modified to give an array of C-dots with distinct features.²⁸ They use countless molecular organic precursors which encompass smaller substances such as carbohydrates and more diverse carbon-containing materials such as biomass.²⁹ Compared to top-down synthesis strategies, bottom-up approaches are favoured because of low cost and potential for mass production.³⁰ Previous studies have predominately used commercially available carbon-containing materials as precursors in the preparation of C-dots as optical sensors of 2-NP.²⁰ Commercially available carbon sources such as ethylene diamine tetraacetic acid (EDTA) and glutathione

have been utilised as carbon sources in the synthesis of C-dots used as optical sensors for 2-NP.^{20,31}

Few studies have reported taking advantage of the abundant biomass as carbon sources for the preparation of C-dots and application in the sensing and detection of 2-NP. Recently, there was a preparation of C-dots using bamboo leaves through a thermal pyrolysis synthetic procedure in a muffle furnace.³² The biomass-obtained C-dots displayed excellent photoluminescent characteristics such as a high fluorescence quantum yield of up to 5.18%. The as-prepared C-dots also exhibited high sensitivity and selectivity towards detection of 2-NP achieving a quenching constant of 102 L/mol. In another recent study, C-dots derived from celery leaves showed high selectivity and sensitivity towards sensing of 2-NP and a detection limit of 3.9×10^{-10} M was determined.³¹ Therefore, the use of biomass as precursors for the synthesis of C-dots gives the advantage of low cost and ecofriendliness, and the procedures are easily scalable.

The present work continues the quest to look for alternative sources of precursors in the synthesis of C-dots, especially locally available biomass. This work unveils a facile and environmentally friendly approach with potential scalability for the fabrication of highly luminescent C-dots using locally available agricultural waste as the carbon precursor. Peels from the fruit of *Citrullus vulgaris* were used in the preparation of the C-dots following the green hydrothermal synthetic approach. The utilisation of agricultural waste can help advance a sustainable waste management programme. The as-prepared C-dots exhibited excellent water solubility, low toxicity and good chemical and photostability. Furthermore, the as-prepared C-dots showed high sensitivity and selectivity towards sensing of 2-NP without further modification and functionalisation. This makes the biomass-derived C-dots a good candidate for application in the detection of 2-NP in real samples such as water and soil.

Materials and methods

Reagents and materials

The peels from the fruit of *C. vulgaris* were collected from hawkers selling the melons in the local market of Palapye, Botswana, after the harvest season. Double-deionised water was produced in the Chemistry laboratory using the Milli-Q system and was used throughout this study without any further purification. A 500-mL hydrothermal synthesis autoclave reactor with a Teflon chamber was purchased from Techinstro (Nagpur, India). A dialysis membrane with a flat width of 43 mm, average diameter of 27 mm and molecular weight cut-off (MWCO) of 14 000, potassium phosphate monobasic ($\geq 99.0\%$), potassium dibasic ($\geq 98.0\%$), anthracene ($\geq 97.0\%$), 2-NP ($\geq 99.0\%$) and dinitrophenylhydrazine ($\geq 97.0\%$) were all purchased from Sigma Aldrich (St Louis, USA). All chemicals used were of analytical grade and used as received without any further purification.

Preparation of carbon dots

The C-dots were synthesised via a simple, green and one-pot hydrothermal synthesis procedure. The fruit of *C. vulgaris* peels was washed with plenty of deionised water, and this process was repeated several times to obtain clean material. The peels were then cut into small pieces and dried in an oven at 60 °C for 36 h. The dried material was then ground into powder using a pestle and mortar. About 2 g of the powder was dissolved into 40 mL of deionised water using a magnetic stirrer for about 10 min. After the complete dissolution of the powder, the solution was then placed into an autoclave and placed in the oven. The time and temperature for the hydrothermal synthesis procedure were varied until an optimum time and temperature of 1 h and 100 °C were achieved. After cooling the solution to room temperature, the resultant solution was then homogenised under sonication (SonicClean, Labotec) for 20 min and placed into a centrifuge (Thermo Scientific, Heraeus, Megafuge 40 Centrifuge) at 8000 rpm for another 20 min. The solution was then filtered using a 0.22- μm syringe filter. The filtered solution was dialysed (retained molecular weight: 14 000 Da) against deionised water for 24 h. The final C-dots light brown solution was stored at 4 °C for further characterisation and application. The synthesis process of the as-prepared C-dots is depicted in Figure 1.

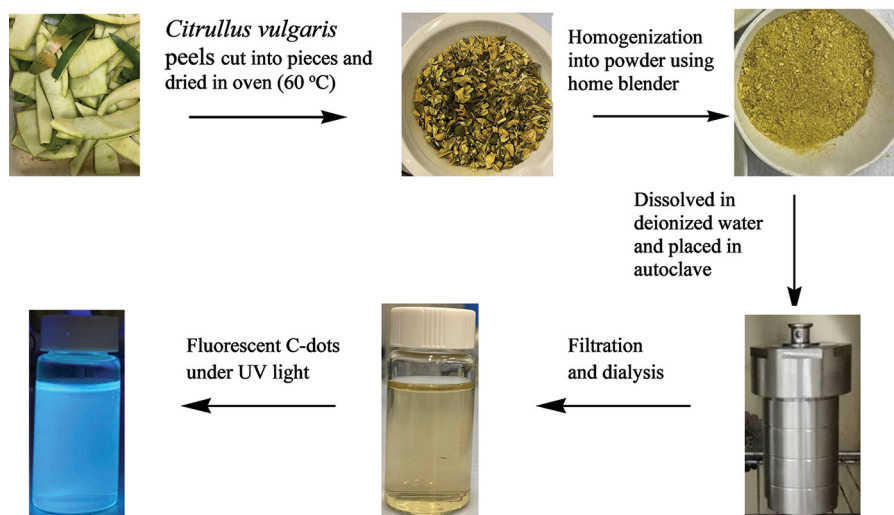


Figure 1: Schematic representation of the preparation of C-dots via the hydrothermal method.

Optimisation of preparation time and temperature

The optimum conditions for the preparation of the C-dots such as time and temperature were determined experimentally. The *C. vulgaris* peels aqueous solutions were subjected to a temperature range of 25–250 °C. The temperature at which the as-prepared C-dots produced the most intense fluorescence was taken as the optimum temperature. Similarly, a time in the range of 0–4 h was selected for the hydrothermal preparation of the carbon dots at a fixed temperature of 100 °C. The optimum C-dots preparation time was taken as the time that resulted in the most intense fluorescence.

Equipment for characterisation of the as-prepared C-dots

The size and morphology of the as-prepared C-dots were determined using an atomic force microscopy (AFM), (Bruker AFM dimension edge in Scan Asyst Peak Force), in the tapping mode. The AFM sample was prepared by placing a drop of the purified C-dots solution on a clean and dry AFM mica slide. The solution was dried at room temperature in a desiccator for 2 h. Fluorescence studies were carried out using a Perkin–Elmer LS 55 spectrofluorometer. All fluorescence measurements were taken at room temperature. The existence of different functional groups on the surface of the as-prepared C-dots was determined using a Thermo Scientific Nicolet iS10 FTIR spectrometer operated at 32 (0.50) cm^{-1} resolution. The FTIR spectra of the pure C-dots were obtained after filtration and dialysis of the aqueous solution. The absorption characteristics of the as-prepared C-dots were established using a Thermo Scientific Evolution 201 UV–Vis spectrophotometer. All the measurements were carried out at room temperature.

Photoluminescent quantum yield of the as-prepared C-dots

The photoluminescent quantum yield (FQY) of the as-prepared C-dots was evaluated using a method reported in the literature.²⁰ The FQY of the as-prepared C-dots was estimated using Equation 1 using anthracene dissolved in ethanol as a reference compound.

$$\phi_{\text{C-dot}} = \phi_{\text{std}} \times \frac{I_{\text{C-dot}} A_{\text{std}} n_{\text{C-dot}}^2}{A_{\text{C-dot}} I_{\text{std}} n_{\text{std}}^2} \quad \text{Equation 1}$$

where $\phi_{\text{C-dot}}$ and ϕ_{std} are the respective photoluminescent quantum yields of the as-prepared C-dots and anthracene standard compound. $I_{\text{C-dot}}$ and $A_{\text{C-dot}}$ represent the integrated fluorescence intensity and absorbance of the as-prepared C-dots whilst $n_{\text{C-dot}}$ is the refractive index of water used to dissolve the C-dots. On the other hand, I_{std} , A_{std} are the integrated fluorescence intensity and absorbance of the anthracene standard material whilst n_{std} is the refractive index of ethanol in which anthracene is dissolved. The FQY of anthracene in ethanol was taken as 0.27 after

excitation at 350 nm as reported in the literature.³³ Anthracene was a preferred reference compound because its emission falls within the range of the emission spectrum of the as-prepared C-dots (360–480 nm). Plots of $I_{\text{C-dot}}$ versus $A_{\text{C-dot}}$ and I_{std} versus A_{std} were made and their slopes were used in the estimation of FQY for the as-prepared C-dots in Equation 1. The absorbance of the as-prepared C-dots and that of the anthracene in the 1 cm cuvette were kept under 0.1 so that suppression of re-absorption effects inside the solutions on the obtained emissions can be achieved.

Optimisation of sensing capability of as-prepared C-dots

Optimisation of conditions for the optical sensing capabilities of the as-prepared C-dots was also carried out. The effect of pH on the photoluminescence properties of the as-prepared C-dots was established. The as-prepared C-dots were dissolved in phosphate buffer in the pH range of 5–13 and the pH at which the fluorescence intensity of the as-prepared C-dots was the highest was taken as the optimised pH for sensing applications.

Procedure for optical sensing of 2-nitrophenol using the as-prepared C-dots

The sensing of 2-nitrophenol was carried out by adding 2.0 mL of varying concentrations of the 2-nitrophenol after dissolution in phosphate buffer (pH 10.0) to 1.0 mL of the as-prepared C-dot contained in a 5.0-mL centrifuge tube. The total volume of the solutions was maintained at 3.0 mL. The solution mixtures were then agitated for 1 min in a multi-pulse vortexer machine and transferred into a quartz cuvette. The fluorescence spectra of the solution mixture were then recorded under the experimentally established excitation wavelength of 400 nm. Method validation was carried out by determining the limit of detection (LOD) and limit of quantification (LOQ) of the as-prepared C-dots towards 2-nitrophenol. Selectivity studies were carried out by introducing potential interferences into the C-dot solution in place of 2-nitrophenol and obtaining the fluorescence spectra.

Results and discussion

Structure and morphological characteristics of the as-prepared C-dots

The particle size, spatial distribution, morphology and crystal lattice of the as-prepared C-dots were explored using an atomic force microscope (AFM) at room temperature. As shown in Figure 2(a) and (b), the C-dots prepared from biomass indicated an amorphous structure with no sign of crystallographic order. The particles are small and irregularly shaped and mainly distributed between 1.7 and 3.0 nm with an average particle size of 2.5 nm (Figure 2(c)). The 2-D and 3-D AFM images (Figure 2(a)

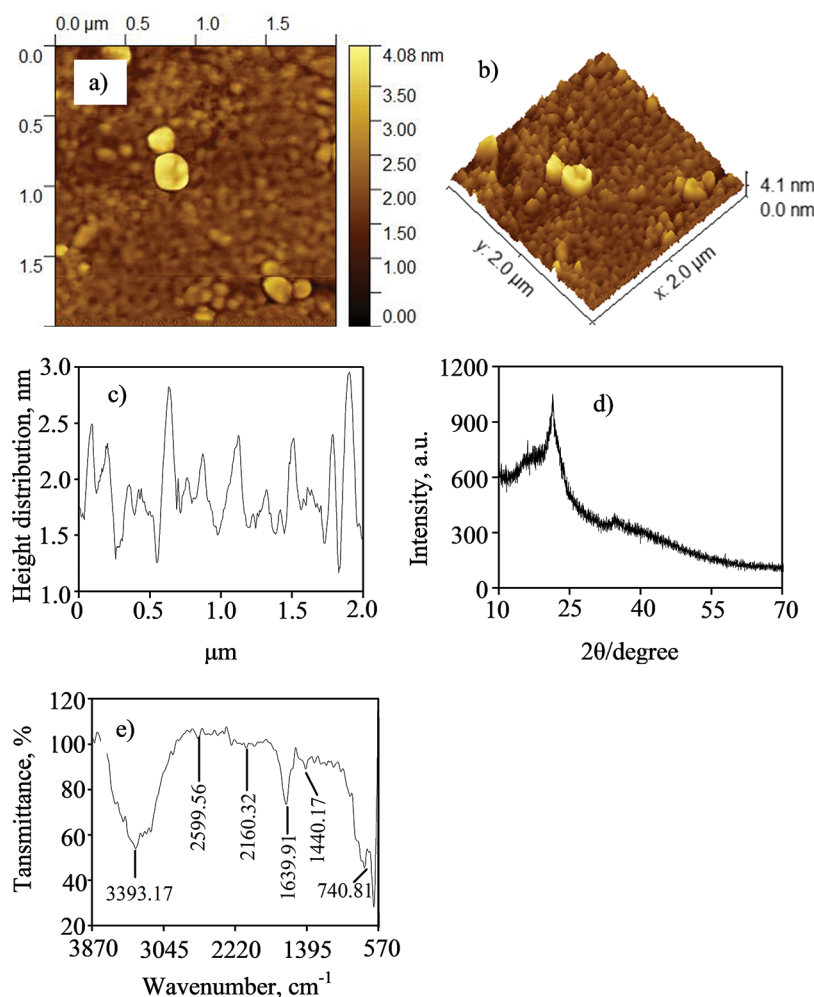


Figure 2: Characterisation of the as-synthesised C-dots using AFM and FTIR: (a) two-dimensional image of the C-dots; (b) three-dimensional image of the C-dots; (c) height distribution of the as-prepared C-dots; (d) XRD pattern of the as-prepared C-dots and (e) FTIR spectrum of the as-prepared C-dots.

and (b)) show that the particles are mono-dispersed with moderate aggregation which indicates good water solubility. The diameter of the C-dots indicates that the nanoparticles comprise several layers, demonstrating graphite-like structure of the C-dots.³⁴ The structural pattern and morphology of the as-prepared C-dots were also studied using the XRD technique. XRD pattern of the as-prepared C-dots exhibits an amorphous carbonaceous core (Figure 2(d)).³⁵ The XRD pattern revealed a distinct peak at $2\theta = 24^\circ$ which suggests intergranular accumulation of carbon atoms in the carbon amorphous phase.³⁶ This confirms the non-crystalline amorphous nature of the C-dots obtained using AFM (Figure 2(a) and (b)). In addition, the peak at $2\theta = 24^\circ$ confirms the graphitic character of the amorphous carbon core.³⁶ The different functional groups present on the surface of the as-prepared C-dots were determined using FTIR. As shown in Figure 2(e), the broad peak centred at 3393 cm^{-1} suggests the presence of the hydroxyl ($-\text{OH}$) and amine ($-\text{NH}$) groups, and the peaks at 1639 cm^{-1} and 1440 cm^{-1} are assigned to the carbonyl ($-\text{C}=\text{O}$) and $\text{C}-\text{N}$ stretching vibrations, respectively. The weak absorption band at 2160 cm^{-1} represents the stretching vibrations of the $-\text{C}-\text{H}$ and $-\text{C}=\text{CH}$.³⁷ In addition, the absorption band at 740 cm^{-1} is assigned to NH_2 wagging band and the bending vibration band of the aromatic $\text{C}-\text{H}$ bond.³⁸ The presence of the hydroxyl and amine functional groups on the surface of the C-dots is responsible for their solubility in water.

Optimisation of hydrothermal synthesis conditions of C-dots

The optimum conditions at which the C-dots revealed the most intense photoluminescence were determined experimentally. The hydrothermal

preparation conditions were based on synthesis time and temperature (Figure 3(a) and (b)). In both cases, the photoluminescence of the as-prepared C-dots was determined at an excitation wavelength of 400 nm . Initially, the fluorescence intensity of the freshly ground *C. vulgaris* peels was determined and revealed very low fluorescence (Figure 3(a); fresh precursor). The hydrothermal synthesis temperature that produced C-dots with the most intense photoluminescence was 100°C after exposing the *C. vulgaris* peels to different temperatures in the range $25\text{--}250^\circ\text{C}$. It should be noticed that the fluorescence intensity of the as-prepared C-dots decreased when the temperature was raised beyond 100°C . A further increase of temperature up to 250°C resulted into complete decomposition of melon peels into ashes instead of the carbon-rich residue. Alternatively, the optimum time required for the hydrothermal synthesis of the C-dots was determined to be 2 h (Figure 3(b)). This is the synthesis time that resulted in the C-dots bearing the most intense photoluminescence. Likewise, increasing synthesis time beyond 2 h caused deterioration of the C-dots photoluminescence (Figure 3(b)). This was due to the complete conversion of the carbon source material into ashes and rather than the carbon-rich nanomaterial.³⁹ Another important point to note is that there is a red shift of the emission wavelength when the synthesis temperature is increased from room temperature to 250°C (Figure 3(a)). A similar observation was made when the synthesis time was increased from 1 h to 4 h (Figure 3(b)). A plausible explanation for the red shift in the emission wavelength is the broad size distribution of the as-prepared C-dots.⁴⁰ C-dots that possess small sizes have been reported to exhibit blue shift emissions whilst larger ones show red shift emissions.⁴⁰ There was no noticeable change in the emission wavelength maxima for C-dots solutions obtained at higher temperatures of 200 and 250°C from that of

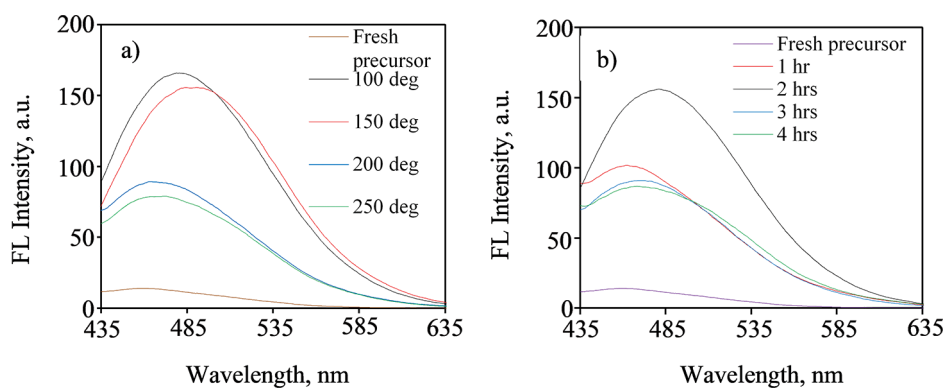


Figure 3: Optimisation of synthesis conditions: (a) fluorescence spectra of the as-prepared C-dots at different synthesis temperature and (b) fluorescence spectra of the as-prepared C-dots at different synthesis times ($\lambda_{\text{ex}} = 400 \text{ nm}$).

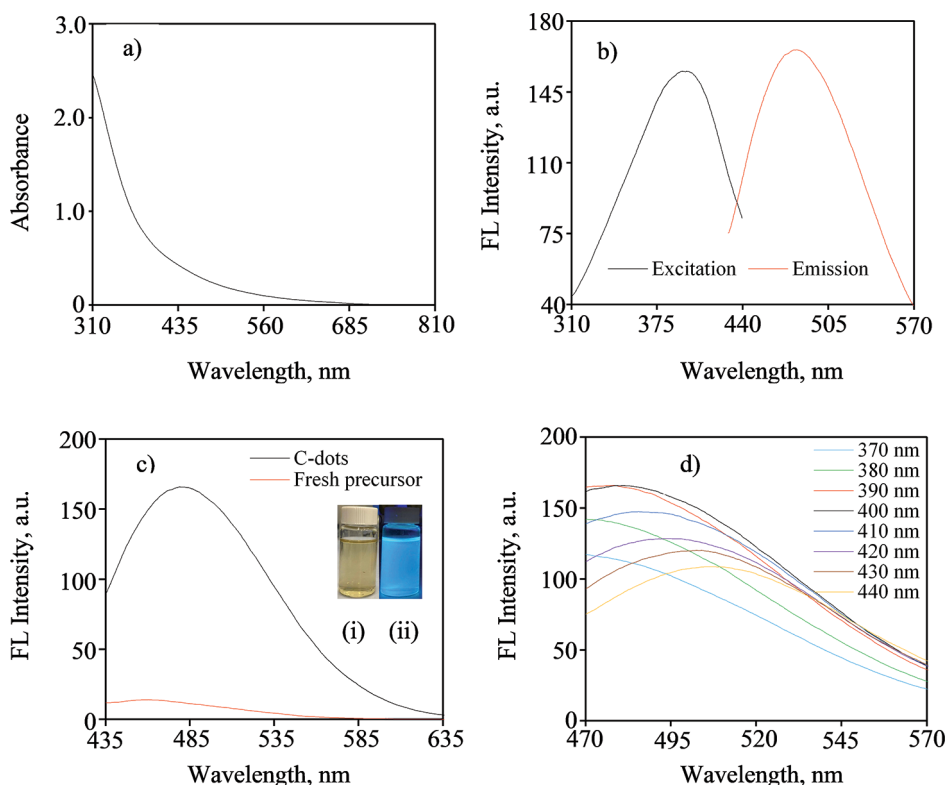


Figure 4: Optical characteristics of C-dots: (a) UV-Vis spectrum of the as-prepared C-dots; (b) excitation-emission spectra of the as-prepared C-dots ($\lambda_{\text{ex}} = 400 \text{ nm}$ and $\lambda_{\text{em}} = 470 \text{ nm}$); (c) emission spectra of the fresh precursor (red curve) and C-dots (black curve) ($\lambda_{\text{ex}} = 400 \text{ nm}$); inset (i) C-dots in deionised water under daylight and (ii) C-dots in deionised water under UV light at 365 nm; and (d) emission spectra of the as-prepared C-dots at different excitation wavelengths ($\lambda_{\text{ex}} = 370\text{--}440 \text{ nm}$).

the fresh precursor. This could be due to the complete decomposition of the precursor instead of the carbon-rich nanomaterial resulting in similar optical characteristics of the decomposed material to that of the starting material.⁴⁰ A similar shift to a longer emission wavelength was observed when heating time of the carbon source material was increased from 1 to 2 h with a more pronounced shift at 2 h. (Figure 3(b)). A small change in the emission wavelength maxima was observed when heating time was increased to 3 h and 4 h, an indication of decomposition of the carbon source material and loss of optical characteristics.

Photoluminescence and absorption properties of the as-prepared C-dots

The absorption spectrum of the C-dots solution derived from *C. vulgaris* peels did not reveal any distinctive sharp peak but rather a broad absorption band in the range of 310–685 nm (Figure 4(a)).

The absence of a distinct absorption peak corroborates the XRD pattern of the possibility of a broad particle size distribution of the as-prepared C-dots.⁴¹ The excitation wavelength (λ_{ex}) responsible for the photoluminescence of the as-prepared C-dots was determined experimentally by running the absorption spectrum of the C-dots using spectrofluorometer (Figure 4(b)). The excitation wavelength that resulted in the most intense fluorescence of the as-prepared C-dots was found to be 400 nm. The emission spectrum revealed a broad peak with an emission wavelength (λ_{em}) maxima of 470 nm and a full width at half maxima (FWHM) of about 100 nm which supports the XRD results of a possible broad particle size distribution of the as-prepared C-dots.⁴² However, the excitation-emission spectra showed a relatively broad Stokes shift of around 70 nm which suggests the photoluminescence of the as-prepared C-dots may be originating from their small emission energy gap and are free from the self-quenching effect (Figure 4(b)).⁴³ As shown in Figure 4(c), the as-prepared C-dots solution exhibited a

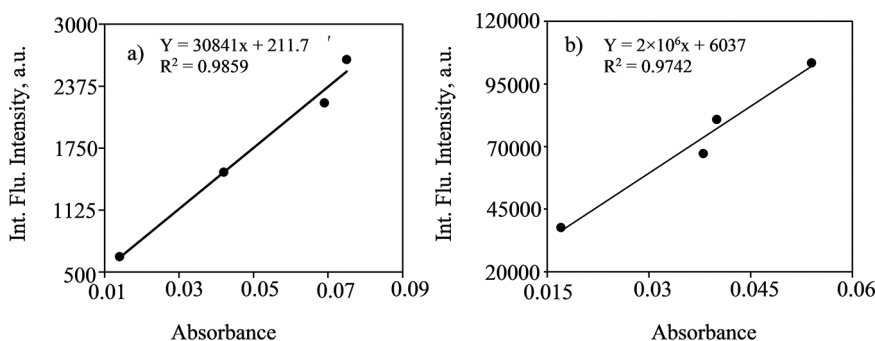


Figure 5: Determination of the fluorescence quantum yield of the as-prepared C-dots. (a) Linear plot of integrated fluorescence intensity versus absorbance for as-prepared C-dots ($\lambda_{\text{ex}} = 400$ nm). (b) Linear plot of integrated fluorescence intensity versus absorbance for the anthracene standard in ethanol ($\lambda_{\text{ex}} = 350$ nm).

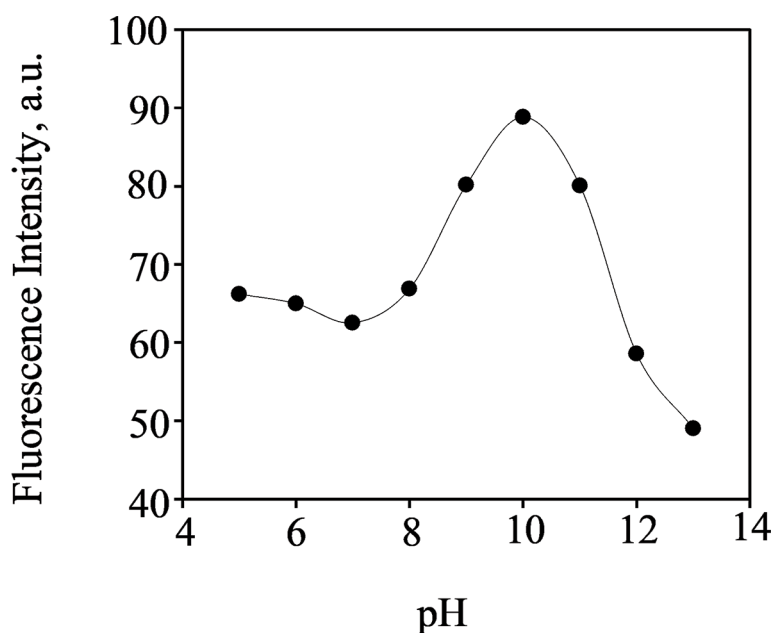


Figure 6: Determination of the effect of pH on the fluorescence intensity of the as-prepared C-dots: $C_{\text{phosphate buffer}} = 0.1$ M; $\lambda_{\text{ex}} = 400$ nm.

bright blue colour under UV irradiation at 365 nm. The inset of Figure 4(c) demonstrates the colour of the as-prepared C-dots solution under daylight (pale brown) and UV lamp at 365 nm (bright blue). It is clear from Figure 4(c) that the as-prepared C-dots exhibit intense fluorescence as compared to the starting material. This implies that hydrothermal heating at optimum conditions of temperature and time results in an efficient and effective carbonisation process through a well-organised structure disintegration and depolymerisation of the precursor carbon polymer sequences into sub-microscopic aggregates.⁴⁰ The photoluminescence properties of the as-prepared C-dots were further investigated by obtaining the emission spectra by varying the excitation wavelength from 370 nm to 440 nm (Figure 4(d)). A red shift in the emission spectra of the as-prepared C-dots was observed as the excitation wavelength was increased progressively from 370 to 400 nm with a concomitant increase in fluorescence intensity. The fluorescence intensities then decreased after excitation at 410–420 nm whilst maintaining a red shift of the emission wavelength. The as-prepared C-dots exhibited the most intense fluorescence after excitation at 400 nm which is in agreement with the excitation-emission spectra in Figure 4(b). A similar pattern of the excitation-dependent fluorescence intensities exhibited by the as-prepared C-dots was observed in a similar study.⁴⁴ The shift in the emission maxima as the excitation wavelength is progressively increased reveals the potential luminescence tuning of the as-prepared C-dots. The excitation-dependent fluorescence of the as-prepared

C-dots that is accompanied by changes in their emission maxima corroborates the XRD and absorption studies of a possible broad particle size distribution and diverse functional groups on the surface states.⁴⁴ In a similar study, the emission maxima occurred at a fixed wavelength when the excitation wavelength was progressively increased from 350 to 450 nm, suggesting that the C-dots synthesised were of high purity and uniform size distribution.³⁸ The optical properties of C-dots have been proposed to emanate from the size of the C-dots, structural defects, aromatic conjugate assembly and the presence of sp^2 sites.³⁶ The fluorescence quantum yield (FQY) of the as-prepared C-dots in aqueous solution (refractive index ~ 1.33) was established experimentally against a reference standard of anthracene exhibiting FQY of 0.27 in ethanol (refractive index ~ 1.36) (Figure 5). The FQY of the as-prepared C-dots was calculated to be 0.40. The low FQY of the as-prepared C-dots can be attributed to the broad particle size distribution.⁴⁵ The FQY of the as-prepared C-dots can be improved through surface passivation and optimisation of other reaction conditions.⁴⁶

Effect of pH on optical properties of C-dots

The effect of pH on the optical characteristics of the as-prepared C-dots was determined experimentally in a pH range of 5–13 using 0.1 M phosphate buffer solutions (Figure 6). The as-prepared C-dots exhibited the most intense fluorescence at pH 10. The fluorescence intensity decreased slightly as the pH was increased from 5 to 7 and

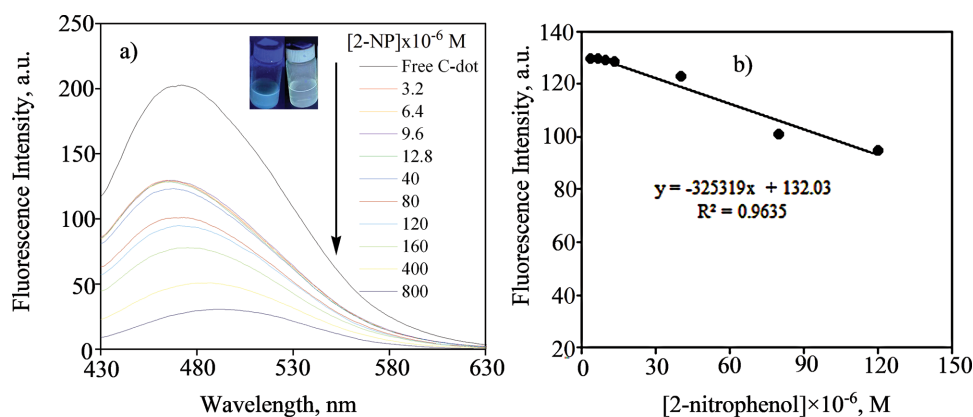


Figure 7: (a) Fluorescence spectra of the as-prepared C-dots in different concentrations of 2-NP in phosphate buffer (pH 10.0). (b) Plot of linear relationship between I and concentration of 2-NP (I = fluorescence of C-dot in the presence of 2-NP). $\lambda_{\text{ex}} = 400$ nm, slit size = 2.5 nm.

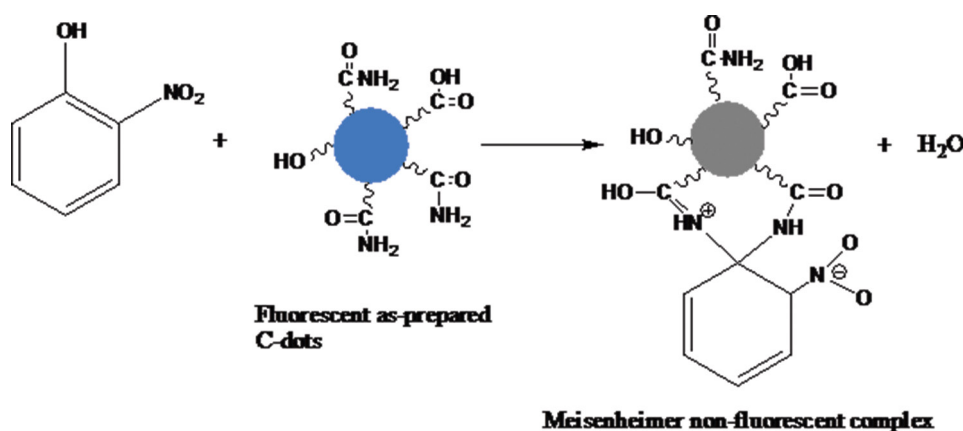


Figure 8: Proposed possible fluorescence quenching mechanism of C-dots in the presence of 2-NP.⁵⁰

then increased substantially from pH 8 reaching a maximum at pH 10. A drastic decrease in the fluorescence intensity was observed between pH 11 and 13. There are several explanations for these observations: firstly, there is the possibility of protonation of functional groups on the surface of C-dots such as carboxyl and amine moieties leading to aggregation which may result in fluorescence quenching of the as-prepared C-dots in highly acidic media.⁴⁷ In more basic conditions (pH 11–13), the presence of hydroxyl anion (OH⁻) leads to the abstraction of the protons from the carboxyl and amine groups forming carboxylate and amide ionic groups which result in the quenching of the fluorescence of the as-prepared C-dots.⁴⁸ Subsequently, the optical sensing studies of the as-prepared C-dots were carried out at an optimal pH of 10.

Application for optical detection of 2-nitrophenol

The intense luminescence of the as-prepared C-dots was exploited towards sensing of the 2-NP explosive additive in phosphate buffer at pH 10. Successive concentrations of 2-NP (0 – 8×10^{-4} M) were added to the C-dots solution (Figure 7(a)). The fluorescence intensity of the C-dots decreased substantially upon the addition of increasing concentrations of 2-NP. A fluorescence quenching efficiency of about 85% was determined after the addition of 8×10^{-4} M of 2-NP to the C-dots solution. In addition, a red shift in the emission wavelength was observed with the concomitant addition of increasing concentrations of 2-NP at a fixed excitation wavelength of 400 nm. The insert of Figure 7(a) shows the visual observation of the quenching efficiency of 2-NP under UV light (365 nm). To obtain a quantitative understanding of the sensitivity of the as-prepared C-dots towards 2-NP, the LOD and LOQ for the explosive additive were determined. A Stern-Volmer plot was obtained, and its slope was used to estimate the LOD and LOQ at λ_{ex} of 400 nm (Figure 7(b)). The LOD and LOQ were, respectively, calculated using the formulae $3\sigma/s$ and $10\sigma/s$ where σ is the standard deviation

of the blank ($n = 6$), obtained from measurement of fluorescence intensities of the as-prepared C-dots in the absence of any analyte and s is the magnitude of the slope of fluorescence intensity versus concentration of 2-NP plot. The as-prepared C-dots were able to detect 2-NP with a linear range of 3.2×10^{-6} to 1.2×10^{-4} M. A low LOD of 2.28×10^{-7} M and LOQ of 7.60×10^{-7} M were calculated for the sensitive optical recognition of the as-prepared C-dots towards 2-NP. The LOD of 2-NP obtained in this study is similar to the results obtained elsewhere for studies of the sensitivity of C-dots towards other nitrophenols.^{20,31,49} An LOD of 7.7×10^{-8} M towards detection of 2-NP was achieved in a previous study where ethylenediaminetetraacetic acid (EDTA.2Na) and urea were used to prepare C-dots under hydrothermal conditions.²⁰ In a similar study, C-dots derived from celery leaves have been reported to detect 2-NP to an LOD of 3.9×10^{-8} M.³¹ This shows that the results obtained in the present study are comparable to those reported in the literature. A possible mechanism for the fluorescence quenching of C-dots by the nitrophenol compounds has been proposed before based on energy transfer action.⁵⁰ An overlap between the maximum absorption band of 2-nitrophenolate ion that is centred at 369 nm and the emission band of the as-prepared C-dots results in a resonant energy transfer process (association quenching).⁵⁰ This mechanism is referred to as competitive absorption or the inner filter effect (IFE).²⁰ The contact quenching is believed to occur via the formation of a spirocyclic zwitterionic Meisenheimer complex.⁵⁰ In such a complex, the negative charge is thought to be delocalised over the nitro group and the cyclohexadienone ring whilst the positive charge is spread over the iminium group (Figure 8).

Interferences from other nitroaromatic and benzene derivatives were evaluated. The fluorescence quenching efficiency was highest for 2-NP compared to all other benzene derivatives studied (Figure 9(a) and (b)). A fluorescence quenching efficiency of 85% for 2-NP was determined

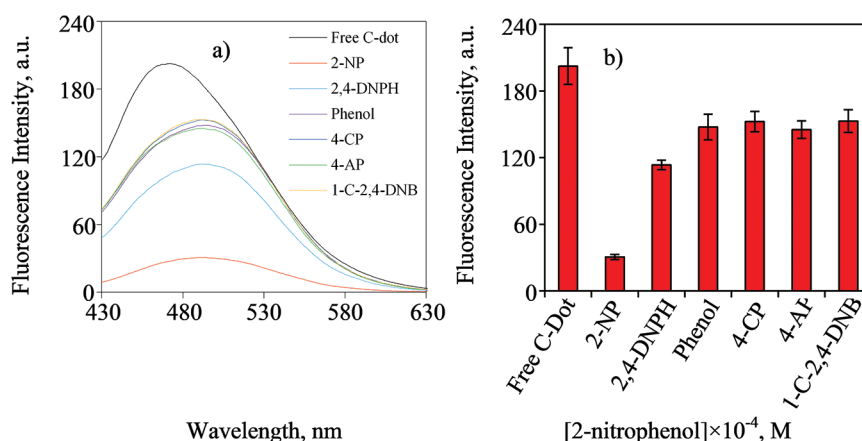


Figure 9: Selectivity studies of the as-prepared C-dots towards 2-NP. (a) Fluorescence spectra of the free C-dots and in the presence of 2-NP and various possible interferences. (b) A plot of fluorescence intensity of free C-dots after the addition of 2-NP and different possible interferences. 2-NP = 2-nitrophenol; 2,4-DNPH = 2,4-dinitrophenylhydrazine; 4-CP = 4-chlorophenol; 4-AP = 4-aminophenol and 1-C-2,4-DNB = 1-chloro-2,4-dinitrobenzene. $\lambda_{\text{ex}} = 400 \text{ nm}$, [Interferent] = $8 \times 10^{-4} \text{ M}$ and [C-dot] = 0.05 g/ml.

whilst the other five benzene derivatives achieved only 24–44% fluorescence quenching efficiency. The low fluorescence quenching efficiencies of the other nitrobenzene and benzene derivatives were observed even after the addition of a large concentration of the possible interferant ($8 \times 10^{-4} \text{ M}$). Contrastingly, 2,4-dinitrophenylhydrazine bearing two nitro groups showed a moderate fluorescence quenching efficiency of about 44%. This could be attributed to the presence of two nitro groups that are electron withdrawing which possibly enhanced the competitive absorption of the nitroaromatic compound against that of the as-prepared C-dots. The as-prepared C-dots displayed excellent selectivity towards 2-NP under controlled conditions of pH 10, and this indicates that the C-dots prepared from biowaste can be used effectively for monitoring 2-NP in aqueous media. This study has shown that *C. vulgaris* peels are not only limited to the synthesis of C-dots and their application towards detection of metal ion and cellular bioimaging^{41,51} or detection of toxic chemicals such as ethyl carbamate in alcoholic beverages⁵² or photocatalytic degradation of methyl orange⁵³ but that they can also be used to prepare C-dots for the detection of toxic environmental pollutants such as 2-nitrophenol in aqueous media. In a previous study, non-environmentally friendly chemicals such as organic solvent, dimethylformamide (DMF), have been used for the synthesis of C-dots and application towards detection of 2-nitrophenol.²⁰ This work rather provided an environmentally friendly alternative for the synthesis of C-dots that are responsive towards the detection of 2-nitrophenol.

Conclusions

In summary, we have synthesised hydroxyl and amide surface-bearing C-dots from *C. vulgaris* biomass as demonstrated by the characterisation studies. The as-prepared C-dots exhibited broad particle size distribution. After optimisation of the synthesis and application conditions, the as-prepared C-dots displayed excellent optical recognition of 2-NP in aqueous media. The effective fluorescence quenching of the C-dots by 2-NP is postulated to occur through energy transfer mechanism. The C-dots prepared from biomass have proven to have potential probes for 2-NP as revealed by their analytical benefits such as quick detection, excellent sensitivity, considerable selectivity and ease of use equipment. The photoluminescence features of the C-dots can be enhanced through surface passivation and functionalisation. This work provides a synthetic approach that is simple, economical, scalable and ecofriendly. Finally, the synthetic strategy of fluorescent C-dots obtained from biomass demonstrates a green approach for converting biowaste into valuable and beneficial optical chemical sensors for environmental pollutants monitoring. The novelty of this research work is the provision of an alternative, cost-effective and ecofriendly method for the potential detection of 2-nitrophenol.

Acknowledgements

We thank the Botswana International University of Science and Technology (BIUST) for the laboratory facilities used for sample analysis.

Competing interests

We have no competing interests to declare.

Authors' contributions

P.D.: Conceptualisation; methodology; student supervision; manuscript writing; data analysis. G.N.P.: Conceptualisation; student supervision; methodology; manuscript writing and revisions. M. M. K.: Data collection; data analysis; writing – initial draft. M. A. B.: Data analysis; manuscript reviewing. M. T.: Materials characterisation; manuscript reviewing. B. P. Materials characterisation; data analysis. J. M.: Conceptualisation; student supervision; methodology; validation; manuscript revisions. R. K.: Materials characterisation, manuscript reviewing.

References

- Singh S. Sensors – An effective approach for the detection of explosives. *J Hazard Mater.* 2007;144:15–28. <https://doi.org/10.1016/j.jhazmat.2007.02.018>
- Yinon J. Field detection and monitoring of explosives. *Trends Anal Chem.* 2002;21(2002):292–301. [https://doi.org/10.1016/S0165-9936\(02\)00408-9](https://doi.org/10.1016/S0165-9936(02)00408-9)
- Kumar D, Elias AJ. The explosive chemistry of nitrogen, a fascinating journey from 9th century to the present. *Resonance.* 2019;24:1253–1271. <https://doi.org/10.1007/s12045-019-0893-2>
- Das P, Mandal SK. Understanding the effect of an amino group on the selective and ultrafast detection of TNP in water using fluorescent organic probes. *J Mater Chem C.* 2018;6:3288–3297. <https://doi.org/10.1039/C7TC05852G>
- Siddique AB, Pramanick AK, Chatterjee S, Ray M. Amorphous carbon dots and their remarkable ability to detect 2,4,6-trinitrophenol. *Sci Rep.* 2018;8:9770. <https://doi.org/10.1038/s41598-018-28021-9>
- Han Y, Chen Y, Feng J, Na M, Liu J, Ma Y, et al. Investigation of nitrogen content effect in reducing agent to prepare wavelength controllable fluorescent silicon nanoparticles and its application in detection of 2-nitrophenol. *Talanta.* 2019;194:822–829. <https://doi.org/10.1016/j.talanta.2018.11.008>
- Alam MK, Rahman MM, Ahmed MAA, Torati SR, Asiri AM, Kim D, et al. Ultra-sensitive 2-nitrophenol detection based on reduced graphene oxide/ZnO nanocomposites. *J Electroanal Chem.* 2017;788:66–73. <https://doi.org/10.1016/j.jelechem.2017.02.004>



8. Adeosun WA, Asiri AM, Marwani HM. Sensitive determination of 2-nitrophenol using electrochemically deposited polymethyl red film for healthcare and environmental safety. *Synth Met.* 2020;261:116321. <https://doi.org/10.1016/j.synthmet.2020.116321>
9. Keith L, Telliard W. ES&T Special report: priority pollutants: I-a perspective view. *Environ Sci Technol.* 1979;13:416–423. <https://doi.org/10.1021/es60152a601>
10. Ammar S, Oturan N, Oturan MA. Electrochemical oxidation of 2-nitrophenol in aqueous medium by electro-fenton technology. *J Environ Eng Manage.* 2007;17:89–96.
11. Scanlon JJ, Falquer PA, Robinson GW, O'Brien GE, Sturrock PE. High-performance liquid chromatography of nitrophenols with a swept-potential electrochemical detector. *Anal Chim Acta.* 1984;158:169–177. [https://doi.org/10.1016/S0003-2670\(00\)84825-4](https://doi.org/10.1016/S0003-2670(00)84825-4)
12. Liu J, Chen Y, Guo Y, Yang F, Cheng F. Electrochemical sensor for o-nitrophenol based on β -cyclodextrin functionalized graphene nanosheets. *J Nanomater.* 2013;2013:632809. <https://doi.org/10.1155/2013/632809>
13. Niazi A, Yazdanipour A. Spectrophotometric simultaneous determination of nitrophenol isomers by orthogonal signal correction and partial least squares. *J Hazard Mater.* 2007;146:421–427. <https://doi.org/10.1016/j.jhazmat.2007.03.063>
14. Chaudhary S, Kumar S, Mehta SK, Ahmad Umar A, Khan MA. Fabrication of water soluble and luminescent Eu_2O_3 nanoparticles for specific quantification of aromatic nitrophenols in aqueous media. *Chem Phys Lett.* 2019;736:136799. <https://doi.org/10.1016/j.cplett.2019.136799>
15. Uddin MT, Alam MM, Asiri AM, Rahman MM, Toupance T, Islam MA. Electrochemical detection of 2-nitrophenol using a heterostructure ZnO/RuO₂ nanoparticle modified glassy carbon electrode. *RSC Adv.* 2019;10:122–132. <https://doi.org/10.1039/C9RA08669B>
16. Deng P, Wang W, Liu X, Wang L, Yan Y. A hydrophobic polymer stabilized CsPbBr₃ sensor for environmental pollutant detection. *New J Chem.* 2021;45:930–938. <https://doi.org/10.1039/D0NJ04498A>
17. Liu GN, Xu RD, Zhao RY, Sun Y, Bo QB, Duan ZY, et al. Hybrid copper iodide cluster-based pellet sensor for highly selective optical detection of o-nitrophenol and tetracycline hydrochloride in aqueous solution. *ACS Sustainable Chem Eng.* 2019;7:18863–18873. <https://doi.org/10.1021/acs.suschemeng.9b03963>
18. Xu X, Ray R, Gu Y, Ploehn HJ, Gearheart L, Raker K, et al. Electrophoretic analysis and purification of fluorescent single-walled carbon nanotube fragments. *J Am Chem Soc.* 2004;126:12736–12737. <https://doi.org/10.1021/ja040082h>
19. Dhenadhayalan N, Lin KC, Saleh TA. Recent advances in functionalized carbon dots toward the design of efficient materials for sensing and catalysis applications. *Small.* 2020;16:1905767. <https://doi.org/10.1002/sml.201905767>
20. Qu Y, Ren G, Yu L, Zhu B, Fang Chai F, Chen L. The carbon dots as colorimetric and fluorescent dual-readout probe for 2-nitrophenol and 4-nitrophenol detection. *J Lumin.* 2019;207:589–596. <https://doi.org/10.1016/j.jlumin.2018.12.017>
21. Wang Y, Hu A. Carbon quantum dots: Synthesis, properties and applications. *J Mater Chem C.* 2014;2:6921–6939. <https://doi.org/10.1039/C4TC00988F>
22. Wang Q, Huang X, Long Y, Wang X, Zhang H, Zhu R, et al. Hollow luminescent carbon dots for drug delivery. *Carbon.* 2013;59:192–199. <https://doi.org/10.1016/j.carbon.2013.03.009>
23. Han Y, Huang H, Zhang H, Liu Y, Han X, Liu R, et al. Carbon quantum dots with photo enhanced hydrogen-bond catalytic activity in aldol condensations. *ACS Catal.* 2014;4:781–787. <https://doi.org/10.1021/cs401118x>
24. Du Y, Guo SJ. Chemically doped fluorescent carbon and graphene quantum dots for bioimaging, sensor, catalytic and photoelectronic applications. *Nanoscale.* 2016;8:2532–2543. <https://doi.org/10.1039/C5NR07579C>
25. Verhagen A, Kelarakis A. Carbon dots for forensic applications: A critical review. *Nanomaterials.* 2020;10:1535. <https://doi.org/10.3390/nano10081535>
26. Roy P, Chen PC, Periasamy AP, Chen YN, Chang HT. Photoluminescent carbon nanodots: Synthesis, physicochemical properties and analytical applications. *Mater Today.* 2015;18:447–458. <https://doi.org/10.1016/j.mattod.2015.04.005>
27. Sun YP, Zhou B, Lin Y, Wang W, Fernando KAS, Pathak P, et al. Quantum-sized carbon dots for bright and colorful photoluminescence. *J Am Chem Soc.* 2006;128:7756–7757. <https://doi.org/10.1021/ja062677d>
28. Crista DMA, Esteves da Silva JCG, Pinto da Silva L. Evaluation of different bottom-up routes for the fabrication of carbon dots. *Nanomaterials.* 2020;10:1316. <https://doi.org/10.3390/nano10071316>
29. Sharma V, Tiwari P, Mobin SM. Sustainable carbon-dots: Recent advances in green carbon dots for sensing and bioimaging. *J Mater Chem B.* 2017;5:8904–8924. <https://doi.org/10.1039/C7TB02484C>
30. Choi Y, Choi Y, Kwon O-H, Kim B-S. Carbon dots: Bottom-up syntheses, properties and light-harvesting applications. *Chem Asian J.* 2018;13:586–598. <https://doi.org/10.1002/asia.201701736>
31. Qu Y, Yu L, Zhu B, Chai F, Su Z. Green synthesis of carbon dots by celery leaves for use as fluorescent paper sensors for the detection of nitrophenols. *New J Chem.* 2020;44:1500–1507. <https://doi.org/10.1039/C9NJ05285B>
32. Yang X, Wang D, Luo N, Feng M, Peng X, Liao X. Green synthesis of fluorescent N,S-carbon dots from bamboo leaf and the interaction with nitrophenol compounds. *Spectrochim Acta A Mol Biomol Spectrosc.* 2020;239:118462. <https://doi.org/10.1016/j.saa.2020.118462>
33. Melhuish WH. Quantum efficiencies of fluorescence of organic substances: Effect of solvent and concentration of the fluorescent solute. *J Phys Chem.* 1961;65(2):229–235. <https://doi.org/10.1021/j100820a009>
34. Bhatt M, Bhatt S, Vyas G, Raval IH, Haldar S, Paul P. Water-dispersible fluorescent carbon dots as bioimaging agents and probes for Hg²⁺ and Cu²⁺ ions. *ACS Appl Nano Mater.* 2020;3:7096–7104. <https://doi.org/10.1021/acsnano.0c01426>
35. Ansi VA, Renuka NK. Table sugar derived carbon dot - a naked eye sensor for toxic Pb²⁺ ions. *Sens Actuators B.* 2018;264:67–75. <https://doi.org/10.1016/j.snb.2018.02.167>
36. Prasannan A, Imae T. One-pot synthesis of fluorescent carbon dots from orange waste peels. *Ind Eng Chem Res.* 2013;52:15673–15678. <https://doi.org/10.1021/ie402421s>
37. Wang BB, Jin JC, Xu ZQ, Jiang ZW, Li X, Jiang FL, et al. Single-step synthesis of highly photoluminescent carbon dots for rapid detection of Hg with excellent sensitivity. *J Colloid Interface Sci.* 2019;551:101–110. <https://doi.org/10.1016/j.jcis.2019.04.088>
38. Dang DK, Sundaram C, Ngo Y-LT, Choi WM, Chung JS, Kim EJ, et al. Pyromellitic acid-derived highly fluorescent N-doped carbon dots for the sensitive and selective determination of 4-nitrophenol. *Dyes Pigm.* 2019;165:327–334. <https://doi.org/10.1016/j.dyepig.2019.02.029>
39. Das P, Ganguly S, Maity PP, Srivastava HK, Bose M, Dhara S, et al. Converting waste *Allium sativum* peel to nitrogen and sulphur co-doped photoluminescence carbon dots for solar conversion, cell labeling, and photobleaching diligences: A path from discarded waste to value-added products. *J Photochem Photobiol B Biol.* 2019;197:111545. <https://doi.org/10.1016/j.jphotobiol.2019.111545>
40. Tan XW, Romainor ANB, Chin SF, Ng SM. Carbon dots production via pyrolysis of sago waste as potential probe for metal ions sensing. *J Anal Appl Pyrolysis.* 2014;105:157–165. <https://doi.org/10.1016/j.jaap.2013.11.001>
41. Zhou J, Sheng Z, Han H, Zou M, Li C. Facile synthesis of fluorescent carbon dots using watermelon peel as a carbon source. *Mater Lett.* 2012;66:222–224. <https://doi.org/10.1016/j.matlet.2011.08.081>
42. Zhi-hao Gao Z-H, Lin Z-Z, Chen X-M, Lai Z-Z, Huang Z-Y. Carbon dots-based fluorescent probe for trace Hg²⁺ detection in water sample. *Sens Actuators B.* 2016;222:965–971. <https://doi.org/10.1016/j.snb.2015.09.032>
43. Ye Q, Yan F, Shi D, Zheng T, Wang Y, Zhou X, et al. N,B-doped carbon dots as a sensitive fluorescence probe for Hg²⁺ ions and 2,4,6-trinitrophenol detection for bioimaging. *J Photochem Photobiol B Biol.* 2016;162:1–13. <https://doi.org/10.1016/j.jphotobiol.2016.06.021>
44. Xu H, Yang X, Li G, Zhao C, Liao X. Green synthesis of fluorescent carbon dots for selective detection of tartrazine in food samples. *J Agric Food Chem.* 2015;63:6707–6714. <https://doi.org/10.1021/acs.jafc.5b02319>
45. Dinake P, Phokedi GN, Janes Mokgadi J, Ntshakisang A, Bothomilwe MA, Kelebemang R, et al. A facile microwave-assisted green synthetic approach of solid-state fluorescent carbon-dot nanopowders derived from biowaste for potential latent-fingerprint enhancement. *Int J Nanosci.* 2021;20:2150051. <https://doi.org/10.1142/S0219581X21500514>



46. Zhuo K, Sun D, Xu P, Wang C, Cao Y, Chen Y, et al. Green synthesis of sulfur- and nitrogen-co-doped carbon dots using ionic liquid as a precursor and their application in Hg²⁺ detection. *J Lumin.* 2017;187:227–234. <https://doi.org/10.1016/j.jlumin.2017.03.022>
47. Yang Z, Xu M, Liu Y, He F, Gao F, Su Y, et al. Nitrogen-doped, carbon-rich, highly photoluminescent carbon dots from ammonium citrate. *Nanoscale.* 2014;6:1890–1895. <https://doi.org/10.1039/C3NR05380F>
48. Sun X, He J, Meng Y, Zhang L, Zhang S, Ma X, et al. Microwave-assisted ultrafast and facile synthesis of fluorescent carbon nanoparticles from a single precursor: Preparation, characterization and their application for the highly selective detection of explosive picric acid. *J Mater Chem.* 2016;4:4161–4171. <https://doi.org/10.1039/C5TA10027E>
49. Tammina SK, Yang Y. Highly sensitive and selective detection of 4-nitrophenol, and on-off-on fluorescence sensor for Cr (VI) and ascorbic acid detection by glucosamine derived n-doped carbon dots. *J Photochem Photobiol A: Chem.* 2020;387:112134. <https://doi.org/10.1016/j.jphotochem.2019.112134>
50. Ahmed GHG, Rosana Badía Laino RB, Calzon JAG, Garcia MED. Highly fluorescent carbon dots as nanoprobe for sensitive and selective determination of 4-nitrophenol in surface waters. *Microchim Acta.* 2015;182:51–59. <https://doi.org/10.1007/s00604-014-1302-x>
51. Rodwihok C, Tam TV, Choi WM, Suwannakaew M, Woo SW, Wongratanaphisan D, et al. Preparation and characterization of photoluminescent graphene quantum dots from watermelon rind waste for the detection of ferric ions and cellular bio-imaging applications. *Nanomaterials.* 2022;12:702. <https://doi.org/10.3390/nano12040702>
52. Han L, Zhu P, Liu H, Sun B. Molecularly imprinted bulk and solgel optosensing based on biomass carbon dots derived from watermelon peel for detection of ethyl carbamate in alcoholic beverages. *Microchim Acta.* 2022;189:286. <https://doi.org/10.1007/s00604-022-05388-1>
53. Ramzilah UR, Aziz A. Removal of methyl orange (MO) using carbon quantum dots (CQDs) derived from watermelon rinds. *Int J Eng Technol Sci.* 2019;6:91–99. <https://doi.org/10.15282/ijets.v6i1.2226>